A Reconfigurable Bandpass Filter for RF/Microwave Multifunctional Systems

Wael M. Fathelbab, *Member, IEEE*, and Michael B. Steer, *Fellow, IEEE*

***Abstract*—A network prototype suitable for reconfigurable filters with imaginary-axis transmission zeros is presented. The prototype is synthesized using classical cascade synthesis. Reconfiguration of the transmission zeros is implemented entirely by tunable capacitors. The measured performance of a narrow-band reconfigurable bandpass filter realized in a planar combline using varactor diodes demonstrates the principle.**

***Index Terms*—Planar combline filters, reconfigurable transmission zeros, tunable capacitors.**

I. Introduction

MODERN communication systems require small, highly selective, and tunable filters [1] with low insertion loss. This has led to the development of sophisticated synthesis techniques [2]–[8] and a wide range of filter prototypes with equiripple in-band and out-of-band amplitude characteristics. Close assignment of transmit and receive bands has resulted in filter specifications that tend to be asymmetric as with transmit/receive diplexers for mobile terminals [12], [13] and base stations [2], [5] of mobile communication systems. In turn, high-performance diplexers are desired with high out-of-band rejection (to satisfy stringent inter-channel isolation) while maintaining low in-band transmit/receive insertion loss. Filters with asymmetric frequency responses are, therefore, favored to those with symmetric characteristics to minimize the number of resonator sections, thus lowering the in-band insertion loss while maintaining a reasonable level of signal rejection.

A multifunctional RF system operating in such an environment requires extra functionality from its active and passive devices. As an example, tunable filter banks are often used to obtain wide-band coverage with the advantage of minimizing overall hardware size. A tunable and reconfigurable filter would be directed at supporting multiple wireless functions using common hardware; hence, decreasing the overall system complexity and potentially improving its performance and functionality. The general class of tunable/reconfigurable bandpass filters would include filters with variable bandwidth, center frequency, skirt selectivity, and group-delay equalization. This paper focuses on the design of reconfigurable filters that alter their transition from passband to stopband by selectively moving finite transmission zero(s) from below or above the passband to the other side. By so doing, the near-in rejection of the filter can be varied appropriately. This functionality is achieved solely through the use of tunable capacitors. An RF multifunctional system utilizing a diplexer made of a pair of reconfigurable bandpass filters will be able to reconfigure its transmission zeros to control its transmit channel receive channel isolation level or to simply notch out-of-band interferers. This extra functionality adds a new feature to systems that are required to adapt to suit their RF environment.

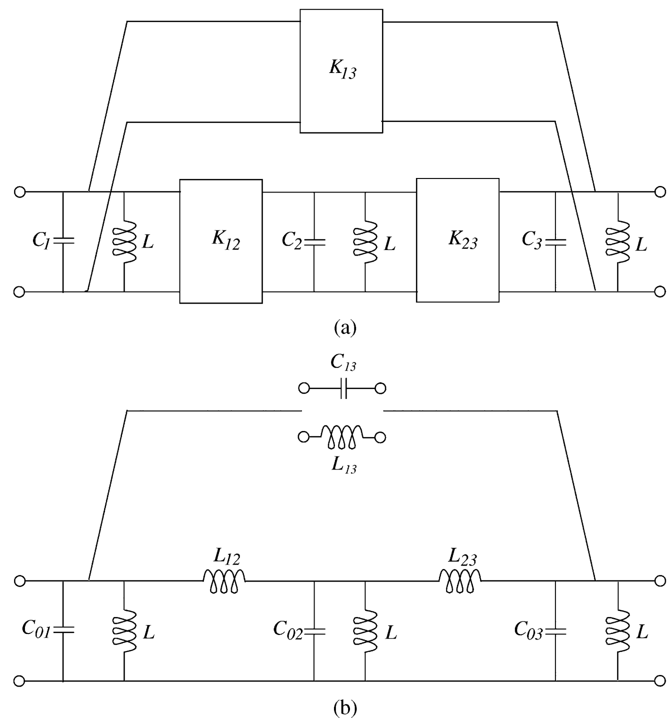

Fig. 1. Bandpass CT realizing a single transmission zero either in the lower or upper stopband: (a) with inter-resonator inverter couplings and (b) with inductive inter-resonator coupling and either inductive or capacitive cross-coupling.

In this paper, a review of the relevant network sections realizing finite frequency transmission zeros is first presented. A suitable prototype for reconfigurable planar filter design is then introduced. Finally, the measured characteristics of a varactor-tuned reconfigurable combline filter suitable for receive applications are reported.

II. Candidate Bandpass Filter Prototypes

The purpose here is to highlight some of the underlying difficulties encountered in implementing tunable/reconfigurable planar filters. Fig. 1(a) shows the cascaded trisection (CT)

Manuscript received February 9, 2004; revised October 14, 2004. This work was supported by the U.S. Army Research Office as a Multidisciplinary University Research Initiative on Multifunctional Adaptive Radio Radar and Sensors under Grant DAAD19-01-1-0496.

The authors are with the Department of Electrical and Computer Engineering, North Carolina State University, Raleigh, NC 27695-7911 USA.

Digital Object Identifier 10.1109/TMTT.2005.843502

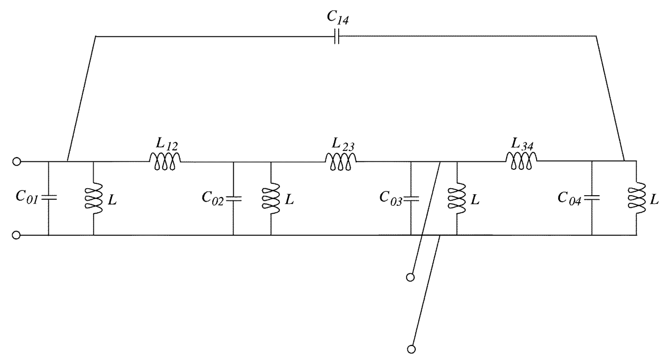

Fig. 2. Bandpass fourth-order network section realizing a single transmission zero either in the lower or upper stopband with inductive inter-resonator coupling and capacitive crosscoupling.

[4]–[6], [11] commonly used in filter prototypes to realize a single imaginary-axis transmission zero. If the crosscoupling inverter has an opposite sign to that of the main line impedance inverters, a transmission zero is placed in the lower stopband, otherwise, if it has the same sign, an upper stopband zero is realized. This implies that a tunable phase shifter in place of the crosscoupling inverter would result in a reconfigurable filter architecture with an increase in overall design complexity. An alternative approximate equivalent to the CT suited for combline realization is shown in Fig. 1(b). In a planar realization, the cross-coupling element may be directly realized in mixed lumped-distributed form [11] provided a tolerable deterioration in stopband performance is accepted. Thus, another possible reconfigurable filter architecture is to use an active switch to interchange between the capacitive and inductive cross-couplings. Passband tunability is usually required in addition to reconfigurability and it is very difficult to design tunable inductors. The need for a switch is also not desirable and the total number of switches required in a filter would be equal to the number of transmission zeros to be realized. A better approach is to achieve reconfigurability by solely using tunable capacitors and, thus, an alternative network section is required. This is shown in Fig. 2. This section has been implemented in the box configuration [2] for base-station filters and is capable of realizing a single imaginary-axis transmission zero either in the lower or upper side of the passband. Upon examining the transmission transfer function of this network section, it can be shown that (with some return-loss degradation) by interchanging the values of the second and fourth capacitors, the location of the transmission zero can be reconfigured from the upper to lower stopband and vice-versa [2]. Consequently, a bandpass filter made of this section has been proposed for complementary transmit/receive diplexers [2] where the bandwidths of the two channels are identical. The key point is that the filter can be reconfigured using only tunable capacitors [2]. The only disadvantage of the network section of Fig. 2 is its complexity. It is of degree 4 and post-tuning and aligning of its response can be problematic for planar realizations. In [2], the box configuration was realized using coaxial resonators where tuning of the inter-resonator couplings was done manually. In Section III, an optimum network section realizing a single imaginary-axis transmission zero is discussed. It will be shown that it is easily realizable in combline with a zero that may be repositioned using tunable capacitors.

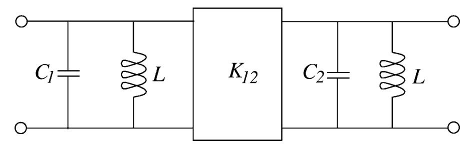

Fig. 3. Pair of bandpass resonators coupled by an impedance inverter.

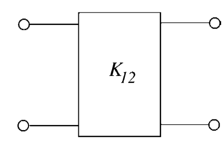

(a)

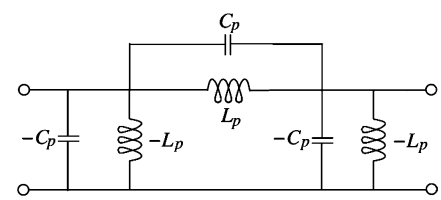

(b)

Fig. 4. Equivalence between: (a) an ideal impedance inverter and (b) its approximate model with an attenuation pole at a finite frequency.

III. Reconfigurable Bandpass Filter Prototype

Consider a pair of resonators coupled by an ideal inverter, as shown in Fig. 3. An ideal impedance inverter has many approximate circuit equivalents [4] among which are the π models with simple elements having a pole at zero or infinity. A more general impedance inverter that has an attenuation pole at a finite frequency [6] rather than at zero or infinity is shown in Fig. 4. This inverter has an attenuation pole at

$$f_p = \pm \frac{1}{2\pi\sqrt{L_p C_p}} \tag{1}$$

and the impedance of the inverter at mid-band is

$$K_{12} = \left(\frac{2\pi f_o L_p}{1 - 4\pi^2 f_o^2 L_p C_p} \right) \tag{2}$$

where f_o is the center frequency.

Substituting (1) into (2) gives

$$K_{12} = \left(\frac{2\pi f_o L_p}{1 - \left(\frac{f_o}{f_p}\right)^2} \right) \tag{3}$$

or

$$K_{12} = \left(\frac{\frac{f_o}{(2\pi C_p f_p^2)}}{1 - \left(\frac{f_o}{f_p}\right)^2} \right). \tag{4}$$

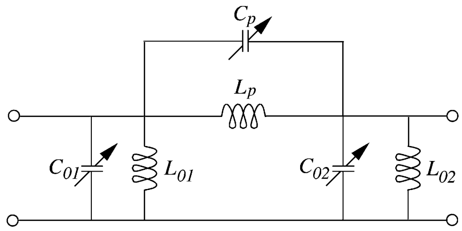

Fig. 5. Pair of bandpass resonators of Fig. 3 with mixed-type coupling.

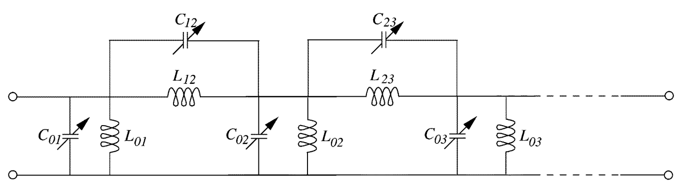

Fig. 6. nth-order filter prototype realizing arbitrarily located transmission zeros with one zero at dc, one zero at infinity, and $(n-1)$ zeros at finite frequencies.

It is seen from (3) and (4) that if the inverter is positive, the pole lies above the passband and, if negative, below [6]. This property is very useful and is key to the design of reconfigurable filters. The negative shunt elements of the approximate inverter can be absorbed into their adjacent neighbors, resulting in the mixed coupled circuit of Fig. 5. This second-order circuit can be directly realized in combline with a series coupling capacitor. If the series and shunt pair of capacitors were tunable then it would be possible to position the finite zero either in the lower or upper stopband. Thus, the design of a reconfigurable filter commences with a prototype representing the filter with transmission zeros in the initial state, and then by tuning relevant capacitors, specific zeros may be reconfigured accordingly. A simple design method [6] is to start from an nth-order prototype with resonators coupled together by ideal inverters and transform, using (1)–(4), as many inverters as required to their corresponding approximates with attenuation poles at finite frequencies. Another more exact method is to use cascade synthesis in the transformed variable [7], [8] to synthesize a network prototype with a specific set of transmission zeros. The general form of an nth-order prototype with $(n-1)$ transmission zeros is shown in Fig. 6 and had been used to realize elliptic function combline filters [9].

A key insight is that, for a specific bandwidth and return-loss level, the reconfigured transmission zeros are restricted to certain locations due to the inter-resonator mixed couplings of the filter that must be same in both states. This dictates the achievable reconfigured locations of the transmission zeros after perturbing the element values of the filter. This is a vital point that requires careful consideration in the design stage in order to satisfy a certain selectivity specification. In Section IV, a reconfigurable filter is implemented.

IV. Filter Implementation

A third-order narrow-band receive filter is constructed on a printed circuit board (PCB). The PCB has a substrate thickness of 62 mil (1.57 mm), relative dielectric constant of 4.7, and loss tangent of 0.016. Using the procedure of [7], the characteristic polynomial $K(S)$ of the filter is constructed with one zero at dc, three zeros at infinity, one finite frequency zero at 735.6 MHz, a center frequency of $f_o = 850$ MHz, bandwidth of 85 MHz, (10% of 850 MHz), and return loss (RL) of 20 dB. This gives

$$K(S) = \frac{\begin{pmatrix} -0.1048970136S^6 & -0.194888590S^4 \\ -0.1201173535S^2 & -0.02456206793 \end{pmatrix}}{(0.001006846557S^3 + 0.0004279173264S)}. \quad (5)$$

The square of the magnitude of the input reflection coefficient is then evaluated from

$$|S_{11}(S)|^2 = \frac{|K(S)|^2}{1+|K(S)|^2} \quad (6)$$

leading to (7), shown at the bottom of this page, from which the input impedance is then found in a 1-Ω system using

$$Z_{\rm in}(S) = \frac{1+S_{11}(S)}{1-S_{11}(S)}. \quad (8)$$

In (5), S is the Richards transform defined as

$$S = j\tan\left(\frac{\pi}{2}\cdot\frac{f}{f_q}\right)$$

with f being the real frequency variable and f_q being the frequency at which the commensurate lines of the prototype are a quarter-wavelength long. For this design, f_q is 2000 MHz, i.e., the resonators are roughly 45° long at the resonant frequency f_o.

A possible prototype obtained by direct synthesis of the input impedance is shown in Fig. 7(a) where the short- and open-circuited stubs represent inductors and capacitors, respectively, at the commensurate frequency f_q. Through application of the Norton's transformation [10], the open-circuited stubs can be distributed throughout the network. Subsequently all the open-circuited stubs have been equated to lumped capacitors at the filter center frequency f_o and, by appropriately scaling the network by a pair of impedance inverters, the transformed prototype of Fig. 7(b) in a 50-Ω system results.

$$S_{11}(S) = \frac{\begin{pmatrix} -0.1048970136S^6 & -0.194888590S^4 \\ -0.1201173535S^2 & -0.02456206793 \end{pmatrix}}{\begin{pmatrix} 0.1048970136S^6 + 0.02586220726S^5 + 0.1980767352S^4 \\ +0.03190556160S^3 + .1220119073S^2 + 0.009656678221S \\ +0.02456206793 \end{pmatrix}} \quad (7)$$

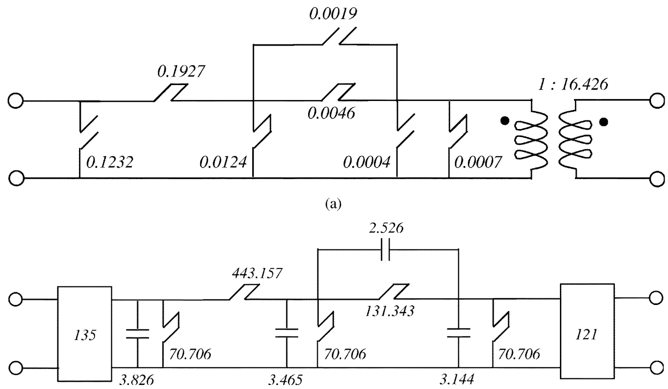

Fig. 7. Distributed bandpass filter prototype with one zero at dc, three zeros at infinity, and one zero at 735.6 MHz. (a) After direct synthesis in a 1-Ω system. (b) After application of suitable circuit transformations and scaling in a 50-Ω system. (All capacitor values are in picofarads.)

From Fig. 7(b), the theoretical capacitor values required for the transmission zero located at 735.6 MHz are

$$\begin{aligned} C_{01} &= 3.826 \text{ pF} \\ C_{02} &= 3.465 \text{ pF} \\ C_{23} &= 2.526 \text{ pF} \\ C_{03} &= 3.144 \text{ pF}. \end{aligned} \tag{9}$$

The value of the impedance inverter with an attenuation pole at 735.6 MHz may now be evaluated from (1) and (3). This is done after approximating the series short-circuited stub of impedance Z_o (of the mixed coupling branch) by a lumped inductor L_p at resonance using

$$jZ_o \tan\left(\frac{\pi}{2} \cdot \frac{f_o}{f_q}\right) = j2\pi f_o L_p. \tag{10}$$

This yields a value of L_p equal to 19.387 nH. However, this step causes a slight shift in the location of the transmission zero, which may be compensated for by fine tuning the parallel capacitor C_{23} from a value of 2.526 pF to 2.414 pF. By referring to Fig. 4(b), C_{23} becomes C_p. From (1), f_p is 735.6 MHz, and from (3), K_{12} is -308.872 Ω. Now, in order to reconfigure the zero to a location in the upper stopband, the absolute value of the inverter must remain the same, but its phase must be altered from 90° to 270°, i.e., effectively changing sign. The new zero location f_p is determined from (3) as follows:

$$308.872 = \left(\frac{2\pi(850 \text{ MHz})(19.387 \text{ nH})}{1 - \left(\frac{850 \text{ MHz}}{f_p}\right)^2} \right) \tag{11}$$

to give a value of 1042.517 MHz. This is essentially achieved by a new capacitance value of C_p (evaluated from (1) at the new frequency, f_p in megahertz) equal to 1.202 pF. With the knowledge of the new value of C_p, the neighboring capacitors (C_{02}, C_{03}) may now be readily found. With very little circuit optimization, the new zero is finally located at 1016.25 MHz, resulting in the following capacitor values:

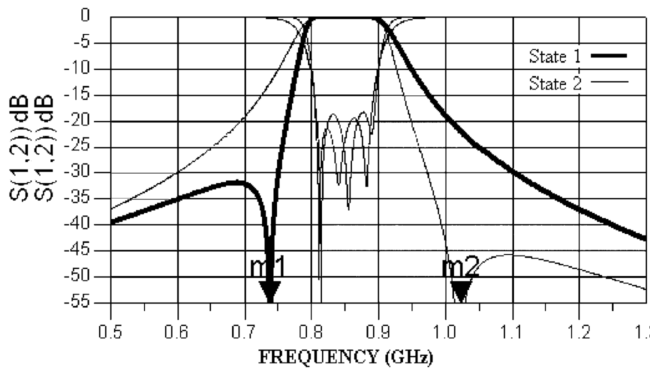

Fig. 8. Simulated lossless responses of the prototype of Fig. 7(b) in two states for the same inter-resonator couplings and RL level. (m1: 735.6 MHz; m2: 1016.25 MHz).

$$\begin{aligned} C_{01} &= 3.886 \text{ pF} \\ C_{02} &= 4.317 \text{ pF} \\ C_{23} &= 1.162 \text{ pF} \\ C_{03} &= 3.718 \text{ pF}. \end{aligned} \tag{12}$$

It is seen from (12) that the value of C_{01} remained virtually unchanged, implying that a total of three capacitors are only required to be tuned to reconfigure the transmission zero. The original (State 1) and reconfigured (State 2) responses are shown in Fig. 8. At this point, a pair of CT filters were synthesized in a 50-Ω system realizing the same transmission zeros as above (i.e., 735.6 and 1016.25 MHz). The element values corresponding to Fig. 1(b) for a lower passband transmission zero are

$$\begin{aligned} C_{01} &= C_{03} = 29.171 \text{ pF} \\ C_{02} &= 36.682 \text{ pF} \\ C_{13} &= 1.84 \text{ pF} \\ L &= 1.2172 \text{ nH} \\ L_{12} &= L_{23} = 10.609 \text{ nH} \end{aligned} \tag{13}$$

and those of upper passband transmission zero are

$$\begin{aligned} C_{01} &= C_{03} = 32.931 \text{ pF} \\ C_{02} &= 34.332 \text{ pF} \\ L_{13} &= 43.875 \text{ nH} \\ L &= 1.2172 \text{ nH} \\ L_{12} &= L_{23} = 10.609 \text{ nH}. \end{aligned} \tag{14}$$

Equations (13) and (14) suggest that all the three shunt capacitors of a CT filter must be tuned. This is in addition to interchanging between capacitive and inductive cross-coupling elements to fully reconfigure the transmission zero, highlighting the benefits of utilizing the filter prototype of Fig. 7 with direct and mixed inter-resonator couplings.

The prototype of Fig. 7(b) was then converted into a physical combline filter using a commercial computer-aided design

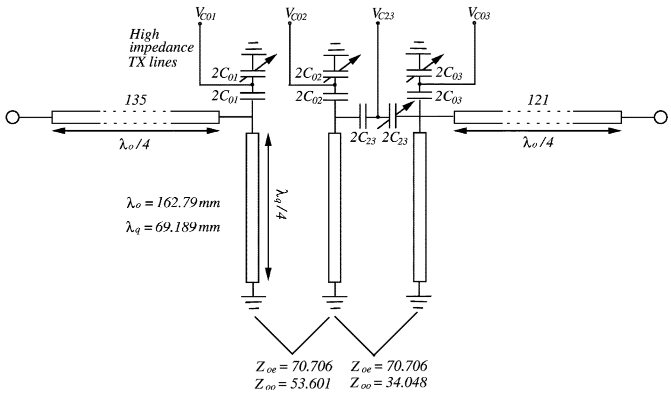

Fig. 9. Layout of combline filter based on the prototype of Fig. 7(b) with bias arrangement. (Half of the capacitors are tunable.)

(CAD) tool.[1] Fig. 9 depicts the layout of the combline filter with even- and odd-mode impedances of each coupled-line sections. All the capacitors of the combline filter were then split into two and connected to high-impedance quarter-wavelength bias lines loaded by low-impedance dc power sources. Initially high-Q lumped capacitors ($Q_C = 65$) were used and the response was reconfigured by manually replacing the lumped capacitors with different values. The practical capacitor values for the transmission zero located at 735.6 MHz are

$$\begin{aligned} C_{01} &= 4.3 \text{ pF} \\ C_{02} &= 3.3 \text{ pF} \\ C_{23} &= 3.3 \text{ pF} \\ C_{03} &= 3.9 \text{ pF} \end{aligned} \tag{15}$$

and for a repositioned zero at 997 MHz (instead of 1016.25 MHz) are

$$\begin{aligned} C_{01} &= 4.4 \text{ pF} \\ C_{02} &= 4 \text{ pF} \\ C_{23} &= 1.4 \text{ pF} \\ C_{03} &= 4.4 \text{ pF}. \end{aligned} \tag{16}$$

These values differ slightly from their theoretical counterparts (9) and (12) due to the microstrip vias on the PCB that were assumed ideal in the simulation and the slight offset in the repositioned zero location in State 2. The capacitances values in (15) and (16) suggest a maximum capacitance ratio for C_{23} of 2.3 : 1 (3.3/1.4) to achieve reconfigurability.

Half of the lumped capacitors were then replaced by varactor diodes with capacitance ratios of 10 : 1[2] to fully construct the reconfigurable filter (see Fig. 9). This was done to boost the effective Q of the series connection of capacitors. The varactor diodes offered a Q of approximately 12 at 850 MHz while the lumped capacitors had a Q of 65 at 850 MHz and, thus, the effective Q of the combination was approximately 20. Since half of the total number of capacitors were replaced by varactor diodes, the maximum tuning ratio required by capacitor $2C_{23}$ calculated

[1]Advanced Design Tool (ADS), ver. 2003A, Agilent Technol., Palo Alto, CA, 2003.

[2]Silicon tuning diodes, Infineon Technol., 2005.

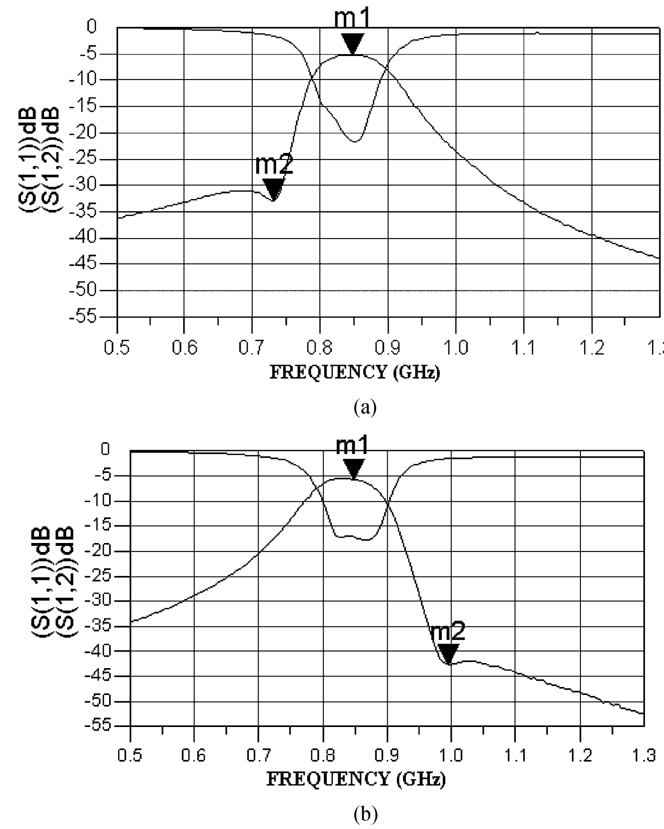

Fig. 10. Measured scattering parameters of reconfigurable filter with a finite transmission zero: (a) in the lower stopband (m1: 850 MHz, −5.253 dB; m2: 732 MHz, −33.027 dB) and (b) in the upper stopband (m1: 850 MHz, −5.753 dB; m2: 996 MHz, −42.785 dB).

from (15) and (16) is now 3.71 : 1. The measured response of the reconfigurable filter in the two states is shown in Fig. 10. In both states, the mid-band insertion-loss level is below 6 dB and it is seen that the filter could be reconfigured to achieve two different selectivity specifications as required.

V. Discussion and Conclusion

A theoretical investigation into the design of a sub-class of reconfigurable filters has been carried out. A practical implementation of a planar microstrip filter has validated the presented design approach. The design theory is based on a network prototype realizing an asymmetric transfer function with possible mixed-coupling branches between adjacent resonators. This circumvents the problem that would exist otherwise where the reconfigurable functionality presented here would be achieved by switching between capacitive and inductive elements or by using tunable phase shifters. Reconfiguring the transmission zeros of the filter enhances the steepness of its response on one side or the other of the passband to suit advanced filtering requirements for multifunctional systems.

References

[1] I. C. Hunter and J. D. Rhodes, "Electronically tunable microwave bandpass filters," *IEEE Microw. Theory Tech.*, vol. MTT-30, no. 9, pp. 1354–1360, Sep. 1982.

[2] R. J. Cameron, A. R. Harish, and C. J. Radcliffe, "Synthesis of advanced microwave filters without diagonal cross-couplings," in *IEEE MTT-S Int. Microwave Symp. Dig.*, 2002, pp. 1437–1440.

[3] R. J. Cameron, "General prototype network synthesis methods for microwave filters," *Eur. Space Agency J.*, vol. 6, pp. 193–206, 1982.
[4] I. Hunter, *Theory and Design of Microwave Filters*. London, U.K.: IEE, 2001.
[5] R. Hershtig, R. Levy, and K. Zaki, "Synthesis and design of cascaded trisection (CT) dielectric resonator filters," in *Proc. 27th Eur. Microwave Conf.*, 1997, pp. 784–791.
[6] R. Levy and P. Petre, "Design of CT and CQ filters using approximation and optimization," *IEEE Microw. Theory Tech.*, vol. 49, no. 12, pp. 2350–2356, Dec. 2001.
[7] H. J. Orchard and G. C. Temes, "Filter design using transformed variable," *IEEE Trans. Circuit Theory*, vol. CT-15, no. 12, pp. 385–408, Dec. 1968.
[8] R. J. Wenzel, "Synthesis of combline and capacitively loaded interdigital bandpass filters of arbitrary bandwidth," *IEEE Microw. Theory Tech.*, vol. MTT-19, no. 8, pp. 678–686, Aug. 1971.
[9] R. Levy and J. D. Rhodes, "A comb-line elliptic filter," *IEEE Microw. Theory Tech.*, vol. MTT-19, no. 1, pp. 26–29, Jan. 1971.
[10] A. I. Zverev, *Handbook of Filter Synthesis*. New York: Wiley, 1967.
[11] J. G. Hong and M. K. Lancaster, *Microstrip Filters for RF/Microwave Applications*. New York: Wiley, 2001.
[12] P. L. Field, I. C. Hunter, and J. G. Gardiner, "Asymmetric bandpass filter using a novel microstrip circuit," *IEEE Microw. Guided Wave Lett.*, vol. 2, no. 6, pp. 247–249, Jun. 1992.
[13] ——, "Asymmetric bandpass filter using a ceramic structure," *IEEE Microw. Guided Wave Lett.*, vol. 2, no. 9, pp. 361–363, Sep. 1992.

Wael M. Fathelbab (M'03) received the Bachelor of Engineering (B.Eng.) and Doctor of Philosophy (Ph.D.) degrees from the University of Bradford, Bradford, U.K., in 1995, and 1999 respectively.

From 1999 to 2001, he was an RF Engineer with Filtronic Comtek (U.K.) Ltd., where he was involved in the design and development of filters and multiplexers for various cellular base-station applications. He was subsequently involved with the design of novel RF front-end transceivers for the U.K. market with the Mobile Handset Division, NEC Technologies (U.K.) Ltd. He is currently a Research Associate with the Department of Electrical and Computer Engineering, North Carolina State University, Raleigh. His research interests include network filter theory, synthesis of passive and tunable microwave devices, and the design of broad-band matching circuits.

Michael B. Steer (S'76–M'82–SM'90–F'99) received the B.E. and Ph.D. degrees in electrical engineering from the University of Queensland, Brisbane, Australia, in 1976 and 1983, respectively.

He is currently a Professor with the Department of Electrical and Computer Engineering, North Carolina State University, Raleigh. In 1999 and 2000, he was a Professor with the School of Electronic and Electrical Engineering, The University of Leeds, where he held the Chair in microwave and millimeter-wave electronics. He was also Director of the Institute of Microwaves and Photonics, The University of Leeds. He has authored over 260 publications on topics related to RF, microwave and millimeter-wave systems, high-speed digital design, and RF and microwave design methodology and circuit simulation. He coauthored *Foundations of Interconnect and Microstrip Design* (New York: Wiley, 2000).

Prof. Steer is active in the IEEE Microwave Theory and Techniques Society (IEEE MTT-S). In 1997, he was secretary of the IEEE MTT-S. From 1998 to 2000, he was an elected member of its Administrative Committee. He is the Editor-in-Chief of the IEEE TRANSACTIONS ON MICROWAVE THEORY AND TECHNIQUES (2003–2006). He was a 1987 Presidential Young Investigator (USA). In 1994 and 1996, he was the recipient of the Bronze Medallion presented by the Army Research Office for "Outstanding Scientific Accomplishment." He was also the recipient of the 2003 Alcoa Foundation Distinguished Research Award presented by North Carolina State University.